SCIENCE CHINA
Information Sciences

• RESEARCH PAPER •

April 2024, Vol. 67, Iss. 4, 142502:1–142502:9
https://doi.org/10.1007/s11432-023-3913-2

Continuous variable quantum teleportation and remote state preparation between two space-separated local networks

Siyu REN[1,2†], Dongmei HAN[1,2†], Meihong WANG[1,2] & Xiaolong SU[1,2*]

[1]*State Key Laboratory of Quantum Optics and Quantum Optics Devices, Institute of Opto-Electronics, Shanxi University, Taiyuan* 030006*, China;*
[2]*Collaborative Innovation Center of Extreme Optics, Shanxi University, Taiyuan* 030006*, China*

Received 30 June 2023/Revised 11 October 2023/Accepted 9 December 2023/Published online 26 March 2024

Abstract Implementing quantum communication between space-separated local networks is essential for designing global quantum networks. In this study, we propose quantum teleportation and remote state preparation schemes between users of two space-separated local networks established by continuous-variable multipartite entangled states. In the proposed schemes, the quantum nodes belonging to the two distant local networks are first entangled by entanglement swapping, and then quantum communication protocols are realized. We show that quantum teleportation between any two users belonging to space-separated local networks can be realized with the assistance of other users, and squeezed thermal states can be remotely prepared in one local network by performing a homodyne projective measurement on the state in another distant local network. Our results provide a feasible approach for quantum communication between space-separated quantum networks with multipartite entangled states.

Keywords quantum communication, quantum network, quantum teleportation, remote state preparation, entanglement swapping, continuous variable

1 Introduction

Quantum networks enable users to implement quantum communication and distributed quantum computation in a network [1–3]. To date, several quantum networks that enable users to share a secret key, i.e., quantum key distribution networks, have been implemented [4–14]. In addition to these, it is essential to establish quantum networks with entangled states that allow users to implement quantum communication based on entanglement [2]. A natural method for constructing a local quantum network with entanglement is to distribute multipartite entangled state modes to space-separated quantum nodes [15, 16]. A global quantum network can generally be built by connecting space-separated local quantum networks [16,17]. For the local quantum networks established by multipartite entangled states, it has been shown that quantum entanglement swapping between multipartite entangled states provides a feasible method for merging space-separated local networks [18, 19]. If a global quantum network is established, it is urgent and essential to design quantum communication protocols between users of space-separated local networks.

Quantum teleportation is a typical quantum communication protocol that transmits an unknown arbitrary quantum state from one station to another based on distributed quantum entanglement. Quantum teleportation has rapidly progressed toward practical application [20]. For example, quantum teleportation with discrete variables over 2 km in fiber channel [21], 143 km in a free space channel [22], and 1400 km from the satellite to the ground [23] have been realized. Deterministic quantum teleportation of coherent [24–26], squeezed [27, 28], and non-Gaussian states [29, 30] have been experimentally demonstrated for the continuous-variable (CV) system. Recently, CV quantum teleportation has also been

* Corresponding author (email: suxl@sxu.edu.cn)
† Ren S Y and Han D M have the same contribution to this work.

realized in fiber channels with transmission distances of 6 [31] and 10 km [32]. For quantum communication networks, quantum teleportation between any two users in a local quantum network established by a CV tripartite Greenberger-Horne-Zeilinger (GHZ) state can be realized in a collaboration model [15].

Remote state preparation (RSP) is another quantum communication protocol that transmits a known state to a receiver based on shared quantum entanglement [33]. Compared with quantum teleportation, RSP requires less classical information and does not require bell state measurement [33]. As a quantum communication protocol, it is more secure than the direct transmission of a state [34]. Various types of quantum states, such as the single photon state [35], sub-Poissonian state [36], superposition state [37], cat state [38,39], continuous variable qubits [40], non-Gaussian state [41], and squeezed state [34], have been remotely prepared, which are limited to point-to-point quantum communication. It has also been shown that remote preparation of squeezed state based on a CV GHZ state can be realized by homodyne projective measurement [42].

To date, quantum teleportation and RSP have been limited to a local network and/or point-to-point communication. In this study, we propose quantum teleportation and RSP schemes between two space-separated local networks established by CV GHZ states. To implement quantum communication protocols, users belonging to two local networks, A and B, are first merged by quantum entanglement swapping. Then quantum teleportation and RSP are implemented from one user in network A to another in network B. We analyze the quantum teleportation and RSP in three cases where two local networks consisting of two Einstein-Podolsky-Rosen (EPR) entangled states, a CV EPR entangled state and a CV tripartite GHZ state, and two CV tripartite GHZ entangled states. The dependences of the fidelity of the teleported coherent state, average photon number, and squeezing level of the remotely prepared squeezed thermal state on the distance between two local networks are also presented. The results confirm the feasibility of quantum teleportation and RSP between two distant local networks, and this has potential applications in global quantum networks.

2 Principle

2.1 Connection of two local quantum networks by entanglement swapping

In this subsection, we consider quantum communication between one user in network A and another user in network B, where two space-separated local networks, A and B, are established by distributed CV multipartite entangled states consisting of n and m modes, respectively (Figure 1). To implement quantum communication, entanglement among quantum nodes in the two local networks is first established by entanglement swapping. Then, quantum communication between any two quantum nodes belonging to networks A and B is implemented with the assistance of other quantum nodes.

An n-mode CV GHZ state $\int \mathrm{d}x|x,x,x,\ldots,x\rangle$ is the eigenstate with total momentum (phase quadrature) zero $\hat{p}_1+\hat{p}_2+\hat{p}_3+\cdots+\hat{p}_N=0$ and relative positions (amplitude quadratures) $\hat{x}_i-\hat{x}_j=0$ $(i,j=1,2,3,\ldots,N)$ [43,44], where the amplitude and phase quadratures are defined by $\hat{x}=\hat{a}^\dagger+\hat{a}$ and $\hat{p}=i(\hat{a}^\dagger-\hat{a})$, respectively. The EPR entangled state corresponds to the case of $n(m)=2$, which has the quadrature correlation of $\Delta^2(\hat{x}_1-\hat{x}_2)=2\mathrm{e}^{-2r}$ and $\Delta^2(\hat{p}_1+\hat{p}_2)=2\mathrm{e}^{-2r}$, where r is the squeezing parameter. While the tripartite GHZ entangled state, corresponding to the case of $n(m)=3$, has the quadrature correlation of $\Delta^2(\hat{x}_i-\hat{x}_j)=2\mathrm{e}^{-2r}$ $(i,j=1,2,3)$ and $\Delta^2(\hat{p}_1+\hat{p}_2+\hat{p}_3)=3\mathrm{e}^{-2r}$.

Quantum modes of the CV GHZ state prepared in the quantum server are transmitted through fiber channels to space-separated quantum nodes to establish the local networks A and B. The distributed modes in the local networks are expressed by $\hat{A}'_n(\hat{B}'_m)=\sqrt{T}\hat{A}_n(\hat{B}_m)+\sqrt{1-T}(\hat{\nu}+\zeta)$, where $T=10^{-0.2L/10}$ represents the transmission efficiency in the fiber channel with distance of L km between the user and server in a local network, $\hat{\nu}$ represents the vacuum mode introduced by the loss in the fiber channel, and ζ is the excess noise with the variance of δ induced by the scattering in fiber and the jitter of phase locking.

As shown in Figure 1, in the entanglement swapping, one mode from network A, for example, $\hat{A}_1$, is transmitted through the fiber channel to one quantum node of network B, for example, $\hat{B}_1$. The joint measurement is performed on $\hat{A}_1$ and $\hat{B}_1$ and the measurement results are fed forward to the rest quantum nodes in network B [18]. After the entanglement swapping, two local networks are merged into a new network with $n+m-2$ nodes. The transmitted mode is given by $\hat{A}'_1=\sqrt{\eta}\hat{A}_1+\sqrt{1-\eta}(\hat{v}+\zeta)$, where $\eta=10^{-0.2L_{\mathrm{AB}}/10}$ is the transmission efficiency between two local networks separated by the distance

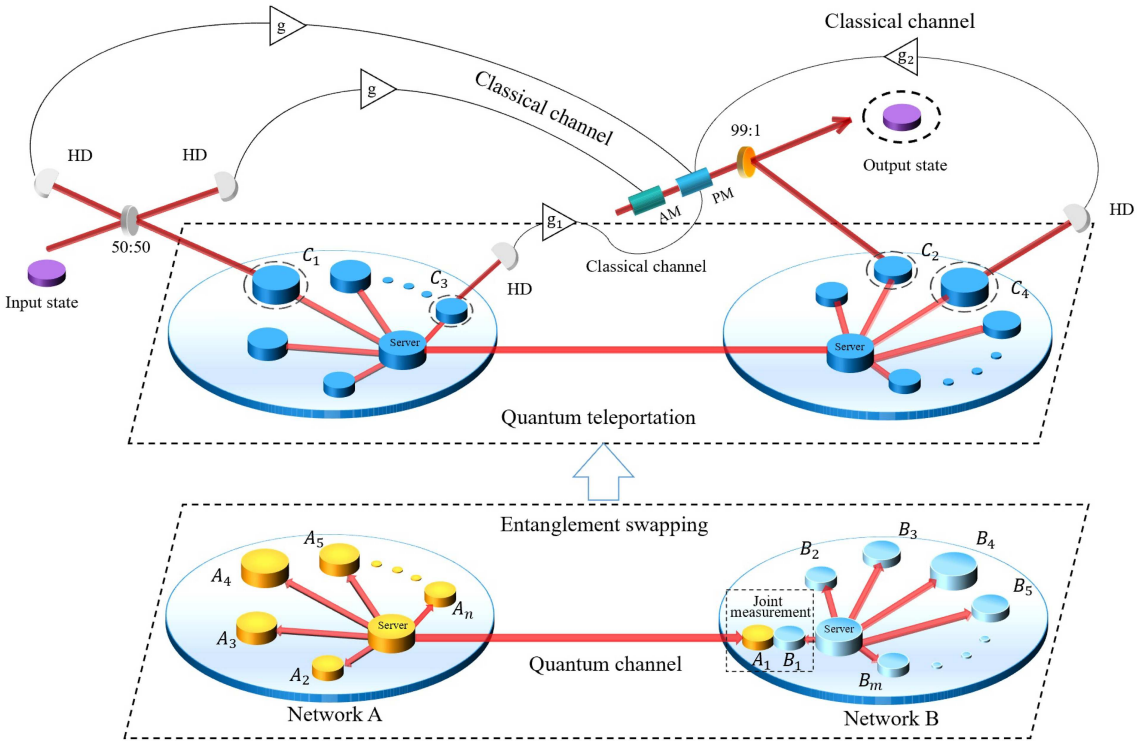

Figure 1 (Color Online) Schematic of quantum teleportation between two users in two local networks. Modes $\hat{A}_1$ and $\hat{B}_1$ are jointly measured to implement entanglement swapping. The remaining modes of $\hat{A}_2\cdots\hat{A}_n$ of Alice's network and $\hat{B}_2\cdots\hat{B}_m$ of Bob's network are entangled after the entanglement swapping. Quantum teleportation from node C_1 to node C_2 of the merged entangled state in case-III is realized with the assistance of the rest nodes C_3 and C_4 in networks A and B. AM: amplitude modulator, PM: phase modulator, HD: homodyne detector.

$L_{\rm AB}$ km.

Here, we take the following three cases as examples to demonstrate the feasibility of our scheme.

Case-I. Two local networks are composed of two EPR entangled states with $n=m=2$ and they are merged into a new EPR entangled state after the entanglement swapping.

Case-II. Two local networks are composed of an EPR entangled state and a tripartite GHZ state with $n=2$ and $m=3$, respectively and they are merged into a new tripartite entangled state after the entanglement swapping.

Case-III. Two local networks are composed of two tripartite GHZ states with $n=m=3$ and they are merged into a new four-partite entangled state after the entanglement swapping.

The details of the entanglement swapping in three cases can be found in Appendix A. In the case of the CV GHZ states with n and m modes in networks A and B, a new CV GHZ state containing $n+m-2$ modes is obtained after the entanglement swapping.

2.2 Quantum teleportation between two local quantum networks

Based on the merged CV GHZ entangled state C, quantum teleportation from one node in network A to one node in network B can be implemented since the entanglement between quantum nodes of two distant local networks has been established. As shown in Figure 1, an unknown input state is coupled with the sender's mode $\hat{C}_i$ on a 50/50 beamsplitter, and the homodyne detection is performed for the output modes of the beamsplitter. The measurement results are given by

$$\hat{x}_u=(\hat{x}_{\rm in}-\hat{x}_i)/\sqrt{2},\quad \hat{p}_v=(\hat{p}_{\rm in}+\hat{p}_i)/\sqrt{2}, \tag{1}$$

where $\hat{x}_i$ ($\hat{p}_i$) is the amplitude (phase) quadrature of the sender's mode and $\hat{x}_{\rm in}$ ($\hat{p}_{\rm in}$) is the amplitude (phase) quadrature of the input state. Then, the measurement results are sent to the receiver's node via classical channels. After receiving the measurement results from the sender, the receiver C_j displaces his mode correspondingly with the assistance of the rest nodes in networks A and B.

In case-I, after entanglement swapping, the two distant local networks are merged into a new EPR entangled state with modes $\hat{C}_1$ and $\hat{C}_2$. Quantum teleportation from C_1 to C_2 can be implemented

directly. After receiving the measurement results, the receiver implements the phase space displacement operation. Therefore, the teleported field can be written as

$$\hat{x}_{\text{tel}} = \hat{x}_2 + \sqrt{2}g\hat{x}_u, \quad \hat{p}_{\text{tel}} = \hat{p}_2 + \sqrt{2}g\hat{p}_v, \tag{2}$$

where g represents the classical gain in quantum teleportation. By substituting (1) into (2) and considering the gain in the classical channel $g = 1$, we can rewrite the teleported field as

$$\hat{x}_{\text{tel}} = \hat{x}_{\text{in}} + (\hat{x}_2 - \hat{x}_1), \quad \hat{p}_{\text{tel}} = \hat{p}_{\text{in}} + (\hat{p}_2 + \hat{p}_1). \tag{3}$$

In the ideal case of infinite squeezing, we obtain $\hat{x}_{\text{tel}} = \hat{x}_{\text{in}}$ and $\hat{p}_{\text{tel}} = \hat{p}_{\text{in}}$, since $\hat{x}_2 - \hat{x}_1 = \hat{p}_2 + \hat{p}_1 = 0$. In the case of finite squeezing and taking the channel parameters into account, the variances of amplitude and phase quadratures of the teleported field are given by

$$\begin{aligned}\sigma^x = \Delta^2\hat{x}_{\text{tel}} =& \cosh 2r(g^2T + \eta G^2 + G^2 + T) - \delta g^2(T-1) - (g^2(T-2)) \\ &- 2G\sqrt{T}(g\sqrt{\eta}+1)\sinh 2r - \delta(\eta-1)G^2 - \eta G^2 + G^2 - \delta(T-1) - T + 1,\end{aligned} \tag{4}$$

$$\begin{aligned}\sigma^p = \Delta^2\hat{p}_{\text{tel}} =& \cosh 2r(g^2T + \eta G^2 + G^2 + T) - \delta g^2(T-1) - (g^2(T-2)) \\ &- 2G\sqrt{T}(g\sqrt{\eta}+1)\sinh 2r - \delta(\eta-1)G^2 - \eta G^2 + G^2 - \delta(T-1) - T + 1,\end{aligned} \tag{5}$$

respectively, where G represents the classical gain of the entanglement swapping and δ represents the variance of excess noise in the fiber channel.

In case-II, after entanglement swapping, two distant local networks are merged into a new CV tripartite entangled state with modes $\hat{C}_1$ and $\hat{C}_3$ in network A, and $\hat{C}_2$ in network B. Quantum teleportation from C_1 to C_2 can be implemented with the assistance of C_3. An unknown state is coupled with mode $\hat{C}_1$, and homodyne detection is performed on the output modes of the beamsplitter. Simultaneously, the phase quadrature of mode $\hat{C}_3$ is measured. To implement quantum teleportation, the results of joint measurement and node C_3 are simultaneously fed forward to C_2 (see Appendix B for detailed analysis). Subsequently, the output state is obtained after the phase space displacement operation.

In case-III, after entanglement swapping, the two distant local networks are merged into a new CV four-partite entangled state with modes $\hat{C}_1$ and $\hat{C}_3$ in network A, $\hat{C}_2$ and $\hat{C}_4$ in network B. For example, quantum teleportation from C_1 to C_2 is implemented with the assistance of C_3 and C_4 (Figure 1). In the teleportation process, the joint measurement results of the input mode and $\hat{C}_1$, as well as the phase quadrature measurement results of $\hat{C}_3$ and $\hat{C}_4$, are fed forward to $\hat{C}_2$, which is realized by simultaneously adding the measurement results of the amplitude and phase quadratures to the amplitude and PMs (see Appendix B for detailed analysis). Consequently, the teleported field at quantum node C_2 is obtained after the phase space displacement operation, which is implemented by using electro-optical modulators and a $99:1$ beam splitter (Figure 1). Here, the $99:1$ beam splitter is used to reduce the loss of the entangled mode introduced by electro-optical modulators, which is widely used for the displacement operation in CV experiments [45,46]. In this case, the $99:1$ beam splitter introduces only 1% loss to the entangled mode (reflecting 99% of the entangled mode and transmitting 1% of the modulated coherent beam). If the reflection of the beam splitter is reduced, more loss is introduced to the entangled mode, which decreases the fidelity of quantum teleportation.

In the case of the CV GHZ states with n and m modes in networks A and B, to implement quantum teleportation between a user (sender) in network A and a user (receiver) in network B, the measurement results of phase quadratures of the rest $n+m-4$ users are simultaneously sent to the receiver in addition to the joint measurement results in the sender's station. After receiving the classical information sent by the sender and other users, the receiver performs a displacement operation on its own optical mode to recover the input state. Thus, quantum teleportation between any two users in networks A and B built by two CV GHZ states with n and m modes can be achieved with the help of other users [43].

2.3 Remote preparation of squeezed thermal state between two distant local networks

To implement RSP between nodes at networks A and B, the two networks are merged into one using entanglement swapping, as presented above. Based on the merged CV GHZ entangled state C, one user measures mode $\hat{C}_i$ originally in network A with an HD and post-selects the measurement results to realize the homodyne projective measurement (Figure 2). If the measurement results at node C_i satisfy

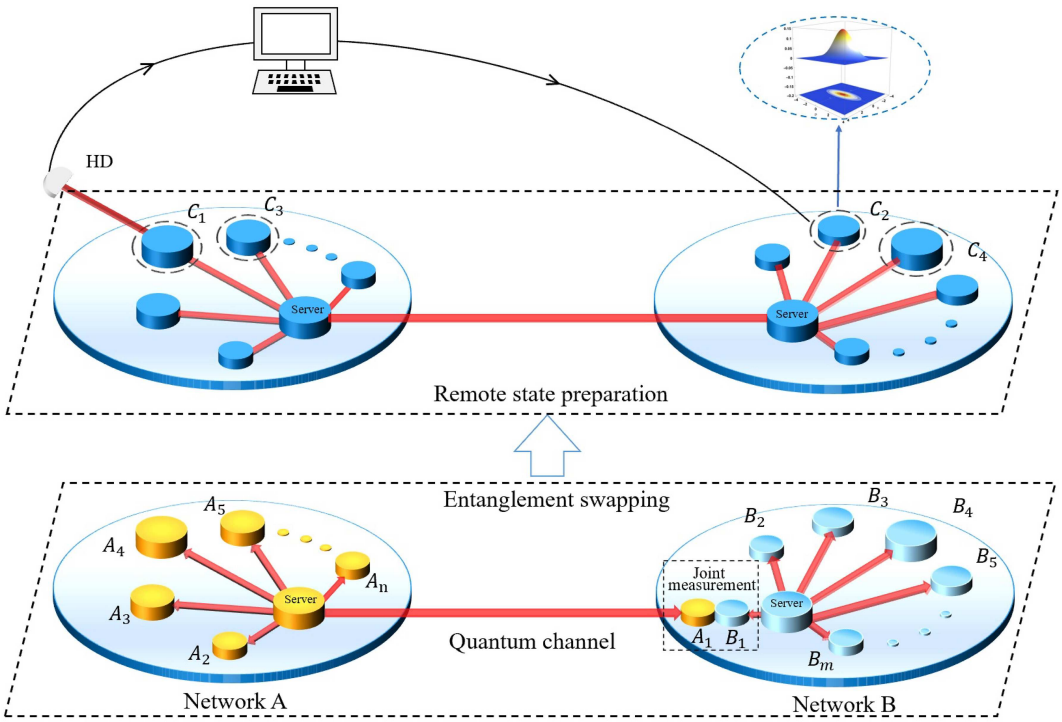

Figure 2 (Color Online) Schematic of RSP between two users in two local networks. Modes $\hat{A}_1$ and $\hat{B}_1$ are jointly measured in the entanglement swapping process. The remaining modes of $\hat{A}_2\cdots\hat{A}_n$ of Alice's network and $\hat{B}_2\cdots\hat{B}_m$ of Bob's network are entangled after the entanglement swapping. A squeezed thermal state can be remotely prepared on node C_2 at Bob's local network by performing the homodyne projective measurement on node C_1 or C_3 at Alice's network. The classical channels from node C_1 (or C_3) to node C_2 are used to transmit the information about the time that the states collapse to squeezed thermal states.

the condition of $x_A = 0$, the users at node C_j in network B record the data and reconstruct the quantum state. The amplitude-squeezed thermal states can be prepared at the remaining nodes of network B [42].

The Wigner function of the merged entangled state C with $k = n + m - 2$ modes is expressed by [47]

$$W(x_{C_1}, p_{C_1}, x_{C_2}, p_{C_2}, \ldots, x_{C_k}, p_{C_k}) = \frac{1}{\sqrt{\mathrm{Det}\sigma}(2\pi)^k} \exp\left\{-\frac{1}{2}\left(\xi^{\mathrm{T}}\sigma^{-1}\xi\right)\right\}, \tag{6}$$

where σ is the covariance matrix of the state C, $\hat{\xi} \equiv (\hat{x}_{C_1}, \hat{p}_{C_1}, \hat{x}_{C_2}, \hat{p}_{C_2}, \ldots, \hat{x}_{C_k}, \hat{p}_{C_k})^{\mathrm{T}}$ is the vector of the amplitude and phase quadratures of the entangled state. The Wigner function of the homodyne projective measurement Π_x on amplitude quadrature of the mode $\hat{C}_1$ is expressed by [48]

$$W[\Pi_x](x_{c_1}) = \delta(x_{c_1} - \alpha), \tag{7}$$

where α is the projective value and it equals zero for the RSP of squeezed thermal states.

In case-I, after entanglement swapping, the modes $\hat{C}_1$ in network A and $\hat{C}_2$ in network B form a CV EPR entangled state. To implement RSP between nodes at networks A and B, homodyne projective measurement is implemented on amplitude quadrature of mode $\hat{C}_1$. Correspondingly, a squeezed thermal state is obtained at node C_2 with the Wigner function expressed by

$$W(x_{C_2}, p_{C_2}) = \int\int \mathrm{d}x_{C_1}\mathrm{d}p_{C_1} W_2 \times W[\Pi_x](x_{C_1}), \tag{8}$$

where W_2 is the Wigner function of the merged EPR entangled state which can be obtained from the covariance matrix of the merged EPR entangled state according to (6).

In case-II, two modes $\hat{C}_1$ and $\hat{C}_3$ in network A and one mode $\hat{C}_2$ in network B form a tripartite GHZ state after the entanglement swapping. To implement RSP between nodes at networks A and B, homodyne projective measurement is implemented on the mode $\hat{C}_1$ (or $\hat{C}_3$). Correspondingly, a squeezed thermal state is obtained at the node C_2 in network B with the Wigner function expressed by

$$W(x_{C_2}, p_{C_2}) = \int\cdots\int \mathrm{d}x_{C_1}\mathrm{d}p_{C_1}\mathrm{d}x_{C_3}\mathrm{d}p_{C_3} W_3 \times W[\Pi_x](x_{C_1}), \tag{9}$$

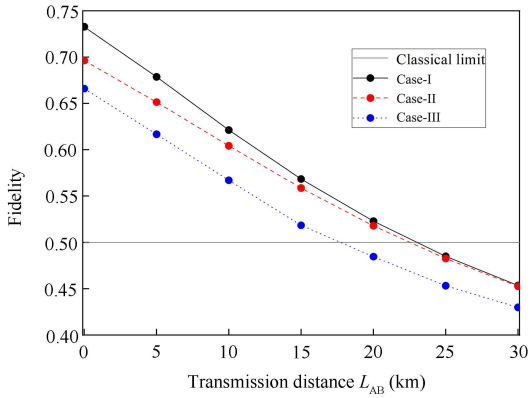

Figure 3 (Color Online) Dependence of fidelity on the transmission distance L_{AB} between two local networks. The black solid, red dashed, and blue dotted curves correspond to case-I, case-II, and case-III of teleportation are based on a merged EPR state, tripartite entangled state, and four-partite entangled state, respectively. The squeezing parameter of the entangled state is $r = 1.15$ and the variance of the excess noise in the fiber is $\delta = 0.01$ in the calculation.

where W_3 is the Wigner function of the merged tripartite entangled state which can be obtained from the covariance matrix of the merged tripartite entangled state.

In case-III, two modes $\hat{C}_1$ and $\hat{C}_3$ in network A and two modes $\hat{C}_2$ and $\hat{C}_4$ in network B form a four-partite CV GHZ state after the entanglement swapping. To implement RSP between nodes at networks A and B, homodyne projective measurement is implemented on the amplitude quadrature of the node C_1 (or C_3). The squeezed thermal state is obtained at node C_2 (or C_4) in network B. The Wigner function of the state at node C_2 is expressed by

$$W(x_{C_2}, p_{C_2}) = \int \cdots \int \mathrm{d}x_{C_1}\mathrm{d}p_{C_1}\mathrm{d}x_{C_3}\mathrm{d}p_{C_3}\mathrm{d}x_{C_4}\mathrm{d}p_{C_4} W_4 \times W[\Pi_x](x_{C_1}), \tag{10}$$

where W_4 is the Wigner function of the merged four-partite entangled state which can be obtained from the covariance matrix of the merged four-partite entangled state.

In the case of the CV GHZ states with n and m modes in networks A and B, to implement RSP between a user in network A and a user in network B, if the homodyne projective measurement is performed on one mode in network A, the $m-1$ modes in network B collapse to squeezed thermal state simultaneously [42]. Therefore, remote preparation of the squeezed thermal state can be achieved between networks A and B built by two CV GHZ states with n and m modes.

3 Results

3.1 Results of the quantum teleportation

The performance of quantum teleportation between space-separated networks A and B is verified by quantum fidelity which quantifies the overlap between the input state and the received state. When a coherent state is the input state, the fidelity of quantum teleportation is given by [24, 26]

$$F = \frac{2}{\sigma_Q} \exp\left[-\frac{2}{\sigma_Q} |v_{\mathrm{in}}|^2 (1-g)^2 \right], \tag{11}$$

where $\sigma_Q = \sqrt{(1+\sigma_W^x)(1+\sigma_W^p)}$ is the variance of the Q function of the teleported field, σ_W^x and σ_W^p are the variances of amplitude and phase quadratures of the output state in the Wigner representation, g is the gain of the classical channel which is chosen to be unit in our calculation and v_{in} is the amplitude of input coherent state.

Here, we consider quantum teleportation between two star-shaped local networks with a radius of $L = 5$ km, i.e., the distances between users and quantum sever are 5 km. Two GHZ entangled states with a squeezing parameter of $r = 1.15$ are produced by quantum servers in the two networks. Figure 3 shows the dependence of fidelities of quantum teleportation on the transmission distance between networks for three cases. For quantum teleportation without entanglement, the corresponding fidelity is 0.5, which is

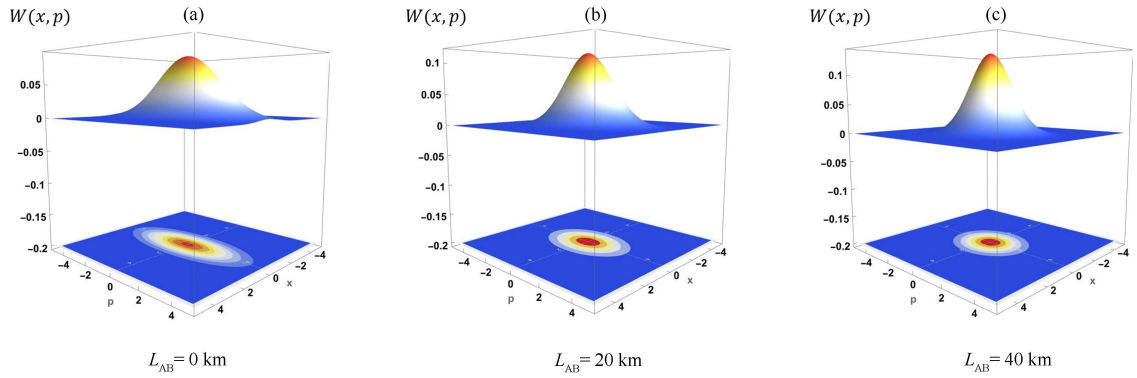

Figure 4 (Color Online) Wigner functions of the squeezed thermal states obtained by the receiver with transmission distances (a) $L_{\rm AB}=0$ km, (b) $L_{\rm AB}=20$ km, and (c) $L_{\rm AB}=40$ km in case-I. The squeezing parameter of the entangled state is $r=1.15$ and the variance of the excess noise in the fiber is $\delta=0.01$ in the calculation.

known as the classical limit. The total distance between two users is $L_T=(L_{\rm AB}+L+L)$ km, where $L_{\rm AB}$ is the distance between two local networks. When the distance $L_{\rm AB}$ is zero, the total distance between two users at nodes C_1 and C_2 is 10 km, and the fidelity for quantum teleportation of a coherent state are 0.74, 0.7, and 0.67 for case-I, case-II, and case-III, respectively. The fidelities of the teleported coherent states decrease with increasing distance between the two local networks. Fidelities of quantum teleportation are below 0.5 when the distances $L_{\rm AB}$ are more than 22, 22, and 17 km for case-I, case-II, and case-III, respectively. This implies that the quantum teleportation of the coherent state between nodes C_1 and C_2 with distances shorter than 32, 32, and 27 km can be realized for the three cases, respectively.

Different user numbers are involved in case-I, case-II, and case-III. It is obvious that the fidelities and transmission distances of the three cases decrease with increasing user numbers in the two local networks. This is mainly because all users are distributed 5 km from the server in the local networks, which decreases the entanglement of the multimode entangled state with the increase in user numbers.

3.2 Results of remote preparation of squeezed thermal states

The performance of RSP between two star-shape local networks is quantified by the squeezing level and average photon number of the remotely prepared squeezed thermal state. The Wigner function of an ideal squeezed thermal state is given by [49]

$$W(x_{C_k},p_{C_k})=\frac{1}{2\pi(1+2\overline{n})}\exp\left\{-\left(\frac{x_{C_k}^2}{\mathrm{e}^{-2r}}+\frac{p_{C_k}^2}{\mathrm{e}^{2r}}\right)/2(1+2\overline{n})\right\},\tag{12}$$

where $\overline{n}$ is the average photon number of a squeezed thermal state. By calculating the fidelity of RSP, i.e., the overlap between the remotely prepared state and an ideal squeezed thermal state, the squeezing level and average photon number are obtained by the maximum fidelity.

For example, in case-I, a squeezed thermal state is obtained at node C_2 in network B by implementing a homodyne projective measurement on node C_1 in network A. Figure 4 shows the Wigner functions of the remotely prepared squeezed thermal states at different transmission distances between two local networks of $L_{\rm AB}=0$ km, $L_{\rm AB}=20$ km, and $L_{\rm AB}=40$ km, corresponding to the total distances between two users of $L_T=10$ km, $L_T=30$ km, and $L_T=50$ km, respectively. It is obvious that the squeezing along the amplitude direction of the remotely prepared state decreases as the transmission distance $L_{\rm AB}$ increases. This is because the shared entanglement between C_1 and C_2 decreases.

Figures 5(a)–(c) show the dependence of the squeezing levels, average photon numbers, and fidelities of the remotely prepared squeezed thermal states on the transmission distance between two local networks. The squeezing levels and average photon numbers are obtained from the maximum fidelity of RSP. A detailed calculation can be found in Appendix C. When the distance $L_{\rm AB}$ is zero, squeezed thermal states with squeezing levels of -3.9, -4.5, and -6 dB and corresponding average photon numbers of 0.35, 0.5, and 0.85 are remotely prepared for case-I, case-II, and case-III, respectively (Figures 5(a) and (b)). As shown in Figure 5(c), the fidelity of the remotely prepared squeezed thermal state is always equal to one at different transmission distances.

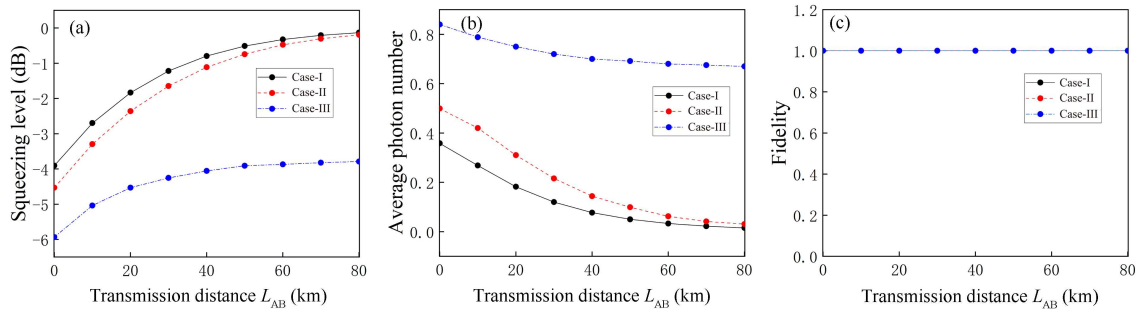

Figure 5 (Color Online) Dependence of (a) squeezing level, (b) average photon number, and (c) fidelity of the remotely prepared squeezed thermal states on the transmission distance between two local networks. The black solid, red dashed, and blue dashed-dotted curves correspond to case-I, case-II, and case-III of RSP are based on a merged EPR state, tripartite entangled state, and four-partite entangled state, respectively. The squeezing parameter of the entangled state is $r = 1.15$ and the variance of the excess noise in the fiber is $\delta = 0.01$ in the calculation.

As the distance between the two local networks increases, the squeezing level of remotely prepared squeezed thermal states decreases. This is because the mode used to perform entanglement swapping involves loss and noise in the fiber channel, which decreases the entanglement. In case-I and case-II, squeezing levels approach zero, and the average photon numbers approach the value of the single mode of the merged entangled state as the distance approaches infinity. In case-III, the squeezing level approaches -4.2 dB, and the average photon number approaches 0.67 as the distance approaches infinity. This is because the state at node C_2 after entanglement swapping is a squeezed thermal state with a squeezing level of -4.2 dB and an average photon number of 0.67.

4 Conclusion

In this study, we propose quantum teleportation and RSP between users of two space-separated local networks established by CV multipartite entangled states. Here, two local networks are first connected by entanglement swapping. These two quantum communication protocols are then realized based on a merged CV EPR entangled state, a merged tripartite CV GHZ entangled state, and a merged four-partite CV GHZ entangled state. We demonstrate that quantum teleportation of a coherent state between any two users of space-separated local networks of a distance of approximately 30 km can be realized, with the assistance of other users. Moreover, we show that remote preparation of squeezed thermal states is achieved between the users from two local networks with a distance of approximately 80 km by performing homodyne projective measurement on the state in one local network. Our results demonstrate the feasibility of quantum teleportation and RSP in merged networks and provide a feasible method for quantum communication between space-separated quantum networks.

Acknowledgements This work was supported by National Natural Science Foundation of China (Grant Nos. 11834010, 62005149), Fundamental Research Program of Shanxi Province (Grant No. 20210302121002), and Fund for Shanxi "1331 Project" Key Subjects Construction.

Supporting information Appendixes A–C. The supporting information is available online at info.scichina.com and link.springer.com. The supporting materials are published as submitted, without typesetting or editing. The responsibility for scientific accuracy and content remains entirely with the authors.

References

1 Kimble H J. The quantum internet. Nature, 2008, 453: 1023–1030
2 Wehner S, Elkouss D, Hanson R. Quantum internet: a vision for the road ahead. Science, 2018, 362: 303
3 Wei S H, Jing B, Zhang X Y, et al. Towards real-world quantum networks: a review. Laser Photon Rev, 2022, 16: 2100219
4 Xu F, Ma X, Zhang Q, et al. Secure quantum key distribution with realistic devices. Rev Mod Phys, 2020, 92: 025002
5 Townsend P D. Quantum cryptography on multiuser optical fibre networks. Nature, 1997, 385: 47–49
6 Elliott C. The DARPA Quantum Network. Boca Raton: CRC Press, 2006
7 Poppe A, Peev M, Maurhart O. Outline of the SECOQC quantum-key-distribution network in vienna. Int J Quantum Inform, 2008, 06: 209–218
8 Wang S, Chen W, Yin Z Q, et al. Field test of wavelength-saving quantum key distribution network. Opt Lett, 2010, 35: 2454
9 Chen T Y, Wang J, Liang H, et al. Metropolitan all-pass and inter-city quantum communication network. Opt Express, 2010, 18: 27217
10 Sasaki M, Fujiwara M, Ishizuka H, et al. Field test of quantum key distribution in the Tokyo QKD network. Opt Express, 2011, 19: 10387

11 Wang S, Chen W, Yin Z Q, et al. Field and long-term demonstration of a wide area quantum key distribution network. Opt Express, 2014, 22: 21739–21756
12 Lancho D, Martinezet J, Elkouss D, et al. QKD in standard optical telecommunications networks. In: Proceedings of International Conference on Quantum Comunication and Quantum Networking, 2010. 142–149
13 Huang D, Huang P, Li H, et al. Field demonstration of a continuous-variable quantum key distribution network. Opt Lett, 2016, 41: 3511–3514
14 Tang Y L, Yin H L, Zhao Q, et al. Measurement-device-independent quantum key distribution over untrustful metropolitan network. Phys Rev X, 2016, 6: 011024
15 Yonezawa H, Aoki T, Furusawa A. Demonstration of a quantum teleportation network for continuous variables. Nature, 2004, 431: 430–433
16 Su X L, Wang M L, Yan Z H, et al. Quantum network based on non-classical light. Sci China Inf Sci, 2020, 63: 180503
17 Ren S Y, Wang Y, Su X L. Hybrid quantum key distribution network. Sci China Inf Sci, 2022, 65: 200502
18 Su X, Tian C, Deng X, et al. Quantum entanglement swapping between two multipartite entangled states. Phys Rev Lett, 2016, 117: 240503
19 Deng X, Tian C, Wang M, et al. Quantification of quantum steering in a Gaussian greenberger-horne-zeilinger state. Optics Commun, 2018, 421: 14–18
20 Hu X M, Guo Y, Liu B H, et al. Progress in quantum teleportation. Nat Rev Phys, 2023, 5: 339–353
21 Marcikic I, de Riedmatten H, Tittel W, et al. Long-distance teleportation of qubits at telecommunication wavelengths. Nature, 2003, 421: 509–513
22 Ma X S, Herbst T, Scheidl T, et al. Quantum teleportation over 143 kilometres using active feed-forward. Nature, 2012, 489: 269–273
23 Ren J G, Xu P, Yong H L, et al. Ground-to-satellite quantum teleportation. Nature, 2017, 549: 70–73
24 Furusawa A, Sorensen J L, Braunstein S L, et al. Unconditional quantum teleportation. Science, 1998, 282: 706–709
25 Bowen W P, Treps N, Buchler B C, et al. Experimental investigation of continuous-variable quantum teleportation. Phys Rev A, 2003, 67: 032302
26 Zhang T C, Goh K W, Chou C W, et al. Quantum teleportation of light beams. Phys Rev A, 2003, 67: 033802
27 Yonezawa H, Braunstein S L, Furusawa A. Experimental demonstration of quantum teleportation of broadband squeezing. Phys Rev Lett, 2007, 99: 110503
28 Takei N, Aoki T, Koike S, et al. Experimental demonstration of quantum teleportation of a squeezed state. Phys Rev A, 2005, 72: 042304
29 Lee N, Benichi H, Takeno Y, et al. Teleportation of nonclassical wave packets of light. Science, 2011, 332: 330–333
30 Takeda S, Mizuta T, Fuwa M, et al. Deterministic quantum teleportation of photonic quantum bits by a hybrid technique. Nature, 2013, 500: 315–318
31 Huo M, Qin J, Cheng J, et al. Deterministic quantum teleportation through fiber channels. Sci Adv, 2018, 4: eaas9401
32 Zhao H, Feng J, Sun J, et al. Real time deterministic quantum teleportation over 10 km of single optical fiber channel. Opt Express, 2022, 30: 3770–3782
33 Lo H K. Classical-communication cost in distributed quantum-information processing: a generalization of quantum-communication complexity. Phys Rev A, 2000, 62: 012313
34 Pogorzalek S, Fedorov K G, Xu M, et al. Secure quantum remote state preparation of squeezed microwave states. Nat Commun, 2019, 10: 2604
35 Lvovsky A I, Hansen H, Aichele T, et al. Quantum state reconstruction of the single-photon Fock state. Phys Rev Lett, 2001, 87: 050402
36 Laurat J, Coudreau T, Treps N, et al. Conditional preparation of a quantum state in the continuous variable regime: generation of a sub-Poissonian state from twin beams. Phys Rev Lett, 2003, 91: 213601
37 Bimbard E, Jain N, Macrae A, et al. Quantum-optical state engineering up to the two-photon level. Nat Photon, 2010, 4: 243–247
38 Ulanov A E, Fedorov I A, Sychev D, et al. Loss-tolerant state engineering for quantum-enhanced metrology via the reverse Hong-Ou-Mandel effect. Nat Commun, 2016, 7: 11925
39 Han D, Sun F, Wang N, et al. Remote preparation of optical cat states based on Gaussian entanglement. Laser Photon Rev, 2023, 17: 2300103
40 Le Jeannic H, Cavaillés A, Raskop J, et al. Remote preparation of continuous-variable qubits using loss-tolerant hybrid entanglement of light. Optica, 2018, 5: 1012
41 Liu S, Han D, Wang N, et al. Experimental demonstration of remotely creating Wigner negativity via quantum steering. Phys Rev Lett, 2022, 128: 200401
42 Han D, Wang N, Wang M, et al. Remote preparation and manipulation of squeezed light. Opt Lett, 2022, 47: 3295–3298
43 van Loock P, Braunstein S L. Multipartite entanglement for continuous variables: a quantum teleportation network. Phys Rev Lett, 2000, 84: 3482–3485
44 van Loock P. Quantum communication with continuous variables. Fortschr Phys, 2002, 50: 1177–1372
45 Takei N, Yonezawa H, Aoki T, et al. High-fidelity teleportation beyond the no-cloning limit and entanglement swapping for continuous variables. Phys Rev Lett, 2005, 94: 220502
46 Su X, Hao S, Deng X, et al. Gate sequence for continuous variable one-way quantum computation. Nat Commun, 2013, 4: 2828
47 Weedbrook C, Pirandola S, García-Patrón R, et al. Gaussian quantum information. Rev Mod Phys, 2012, 84: 621–669
48 Paris M G A, Cola M, Bonifacio R. Remote state preparation and teleportation in phase space. J Opt B-Quantum Semiclass Opt, 2003, 5: 360–364
49 Kim M S, de Oliveira F A M, Knight P L. Properties of squeezed number states and squeezed thermal states. Phys Rev A, 1989, 40: 2494–2503